

Coupled-Inductor-Based DC Current Measurement Technique for Transformerless Grid-Tied Inverters

Ahmed Abdelhakim, *Student Member, IEEE*, Paolo Mattavelli, *Fellow, IEEE*,
Dongsheng Yang, *Member, IEEE*, and Frede Blaabjerg, *Fellow, IEEE*

Abstract—Grid-tied photovoltaic (PV) inverters must fulfill several requirements, including high efficiency and reduced cost and complexity of the overall system. Hence, transformerless operation is advantageous in order to achieve the prior requirements. Meanwhile, such operation results in several demerits, like the dc current component injection into the grid. This component should be effectively mitigated in order to avoid some impacts, like the saturation of the transformers in the distribution network. On the other hand, limiting this component up to few milliamperes is a challenging issue due to the various measurement errors. Accordingly, different blocking and measurement techniques have been proposed and studied to overcome this issue, where some demerits are seen behind each technique like the implementation complexity, the common mode voltage problems, and the high filter requirements. Moreover, none of them measures the dc component directly, but predicts its value using different approaches. Hence, this letter proposes a new technique to measure this dc current component with high accuracy using a coupled-inductor combined with a small range hall effect current sensor in order to achieve the lowest possible cost with the highest possible accuracy. The proposed technique is introduced, analyzed, and tested experimentally to verify its principle of operation. Also experimental measurement of the dc current component using a 5 kVA transformerless grid-tied voltage source inverter (VSI) is introduced with and without the proposed technique in order to validate its operation.

Index Terms—Coupled-inductor; Current sensor; Current transformer; DC current; Grid-tied inverters; Photovoltaic; Renewable energy sources; Transformerless; Voltage source inverter;

I. INTRODUCTION

The use of grid-tied photovoltaic (PV) inverters is continuously increasing and several requirements have to be fulfilled in order to achieve the highest possible performance of the employed power conditioning stage (PCS). Recently, transformerless operation, i.e. eliminating the low frequency power transformer from the grid-tied PV inverter, is followed in order to improve the PCS efficiency and to reduce its cost and volume [1]–[5]. Even though the gained merits from the transformerless operation, it results in several problems, where the dc current component injection into the grid is a major one. This dc current component might exist due to one or more of the following reasons [5]:

Manuscript received April 12, 2017; revised May 7, 2017; accepted June 1, 2017.

A. Abdelhakim and P. Mattavelli are with the Department of Management and Engineering, University of Padova, 36100 Vicenza, Italy (e-mail: ahmed.a.abdelrazek@ieee.org; paolo.mattavelli@unipd.it).

D. Yang and F. Blaabjerg are with the Department of Energy Technology, Aalborg University, 9220 Aalborg, Denmark (e-mail: pda@et.aau.dk, fbl@et.aau.dk).

- an asymmetry in the switching scheme;
- some problems in the gate drive circuits;
- non-identical turning ON and OFF times or voltage drops of the employed switches;
- measurement errors in the employed sensors.

Furthermore, it is of importance to mitigate this dc current component in order to avoid the following impacts [5]–[8]:

- affecting the operating point of the power transformers along the distribution network;
- increasing the system losses due to the circulation between the inverter phase legs or between the paralleled inverters;
- affecting the normal operation of connected ac motors to the line;
- corrosion problems in the grounding wires.

Several standards have been established in order to consider this issue and limit its effect on the power network elements. For example, in the IEEE standard 1547-2003 [9] and the Italian standard CEI 0-21 [10], the injected dc current component shall not exceed 0.5% of the nominal output current, while the Australian standard AS4777.2 [8] has established a limit of 0.5% of the nominal output current or maximum 5 mA. Accordingly, it is a challenging issue to measure such few milliamperes within several tens of amperes due to the measurement accuracy, i.e. very high accuracy current sensor is mandatory, which is usually expensive, especially if the target is to limit the component below the 5 mA limit. Hence, several research activities have been conducted in order to address this issue and fulfill standards requirements. These different research activities have proposed several methods to limit this dc current component by considering a blocking method or a measurement approach combined with a dedicated control scheme. It is worth to note that there are some current sensors with very high accuracy that can be used to detect the dc current component with higher accuracy, but these sensors are usually more suitable for measurement equipment (i.e. it is not usually suitable for the PV application due to the cost constrains).

In literature, two blocking approaches have been introduced in [3], [11] using blocking capacitors. The authors in [3] discussed the effect of using a half-bridge single-phase voltage source inverter (VSI) to block the dc component utilizing the dc link capacitors. Meanwhile, the authors in [11] proposed to use an output series dc capacitor instead of an ac capacitor to achieve the same goal, in which a certain control scheme is utilized in order to control the average voltage across the

output capacitor, in addition to using protective diodes for over and reverse voltages protections. On the other hand, several measurement techniques combined with control algorithms have been introduced as well. In [12], the authors demonstrated how to detect a small level of dc current in the single-phase full-bridge grid-tied inverters. This measurement technique uses a small 1:1 voltage transformer and an RC circuit to detect the dc voltage. It is quite difficult to measure the dc voltage with high accuracy due to the existing ac voltage, which increases in magnitude with the increase of the employed phase shift between the grid and the inverter voltages. On the other hand, the authors in [13], [14] are discussing a measurement technique to detect the dc offset between the inverter output terminals using RC filters and voltage transformers, in which the common mode voltage problems should be effectively considered. Similarly, the authors in [15], [16] are discussing the dc current component measurement and mitigation using output low-pass filters and voltage sensors for single-phase and three-phase systems. Also in [17], the authors are using a reactor with a specific design combined with a current transformer and an LC filter to mitigate the dc component. This reactor is working at the knee point of the magnetizing curve or higher, where this measurement technique is seen as a bulky and complicated one. The authors in [18], [19] are discussing the effect of using means of dc offset calibration on the dc current injection by measuring the dc link current, in which the gain and the linearity errors are neglected and they might affect the measurement in different scenarios.

In addition to the prior mentioned approaches, other techniques have been discussed in [20]–[24]. The authors in [20]–[23] are utilizing means of even harmonic analysis in order to detect small dc offsets and minimize the injected dc current component to the grid. In [24], a simple magnetic circuitry is used to measure the dc current component. This technique utilizes a magnetic core with compensating winding in order to reduce the ac current flux component without influencing the dc flux. Then, a hall sensor is used to measure the dc flux in the core, which is combined with a residual ac flux.

Among the different measurement techniques discussed before, none of them measures the dc current component directly except the technique introduced in [24]. These prior art techniques physically block the dc current component or predict its value from the measured voltage. Hence, this paper is proposing a new measurement technique to mitigate this dc current component. The proposed technique utilizes a 1:1 coupled-inductor combined with a small range current sensor in order to extract this component with the highest possible accuracy and lowest cost and complexity.

The rest of this paper is organized as follows: Section II discusses the proposed technique, showing its principle of operation and its design challenges. The control scheme of a grid-tied voltage source inverter (VSI), including the proposed measurement technique, is introduced in Section III. Finally, experimental results are shown in Section IV, where the results include the obtained dc current component measurement with and without the proposed measurement technique using a 5 kVA transformerless grid-tied VSI.

II. PROPOSED DC CURRENT MEASUREMENT TECHNIQUE

It has been seen that several demerits exist behind the prior mentioned dc current injection blocking and measurement techniques. Furthermore, none of them measures the dc component directly, but predicts its value using different approaches. Hence, this letter proposes another technique by measuring the injected dc current itself, i.e. it does not predict for its value from the equivalent dc voltage. This proposed technique uses a 1:1 coupled-inductor combined with a small range hall effect current sensor in order to extract the dc current as shown in Fig. 1(a).

The principle of operation of this technique, assuming an ideal 1:1 coupled-inductor with a short circuited secondary winding as in Fig. 1(a), can be explained as follows: if the current in the primary winding is i_p , which comprises ac and dc components (i.e. $i_p = i_{ac} + I_{dc}$), then only the ac component (i_{ac}) will be ideally induced in the secondary winding (i.e. $i_s = i_{ac}$). Hence, if both windings are taken through a hall effect current sensor as shown in Fig. 1(a), only the dc component (I_{dc}) will be measured. Note that the ac flux coming out from the primary winding is compensated by the secondary one in the measuring window, resulting in having only the dc flux in the measuring window. Thus, it is possible to use a small range hall effect current sensor and measure the dc component directly with the highest possible accuracy.

The equivalent circuit of a 1:1 coupled-inductor with a short circuited secondary winding, neglecting the core losses, is shown in Fig. 1(b). In steady state, if the primary winding current (i_p) comprises ac and dc components (i.e. $i_p = I_p \angle 0 + I_{dc}$), the secondary winding current (i_s) will include only the ac component (i.e. $i_s = I_s \angle \varphi_s$), which can be calculated by

$$\frac{I_s}{I_p} = \frac{\omega_1 \cdot L_m}{\sqrt{R_s^2 + (\omega_1 \cdot (L_{l_s} + L_m))^2}} \approx \frac{k}{\sqrt{1 + k^2}}, \quad (1)$$

$$\varphi_s = \frac{\pi}{2} - \tan^{-1} \left(\frac{\omega_1 \cdot (L_{l_s} + L_m)}{R_s} \right) = \frac{\pi}{2} - \tan^{-1}(k), \quad (2)$$

where L_m is the magnetizing inductance, L_{l_s} is the secondary leakage inductance, R_s is the secondary winding resistance, including the wiring cable needed to couple the current sensor, ω_1 is the fundamental frequency in rad/s , and k is a factor that describes ideality of the coupled-inductor and it is equal to $(\omega_1 \cdot (L_{l_s} + L_m) / R_s)$. Note that the coupled inductor is an ideal one when $k = \infty$, at which $i_s = i_p$. Thus, the difference between i_p and i_s gives the magnetizing current ($i_m = I_m \angle \varphi_m$), which represents the residual ac component measured by the current sensor with the dc component.

In addition to that, this coupled-inductor introduces additional power losses. These power losses are coming from two sources. The first source of losses is the core loss, which is negligible as the magnetizing current is much smaller than the main primary current with a low frequency dominant component. On the other hand, the second source of losses is the windings losses (P_w), which is equal to $(I_p^2 \cdot R_p + I_s^2 \cdot R_s)$.

In order to achieve the highest possible performance and get close as much as possible to the ideal case introduced in

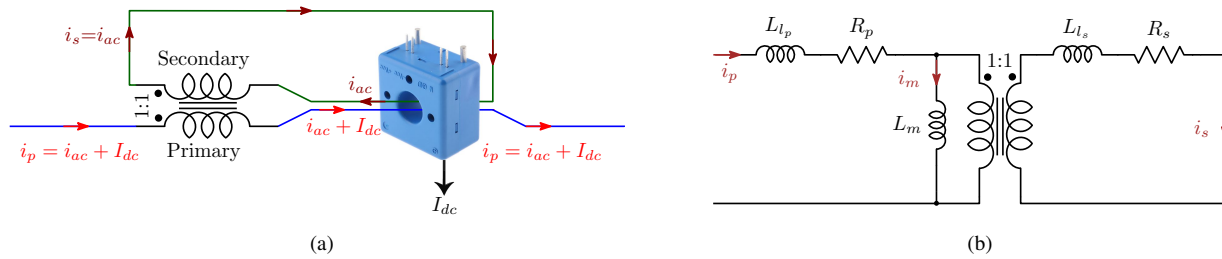


Fig. 1. Proposed coupled-inductor-based dc current measurement technique for grid-tied inverters. (a) principle of operation; (b) equivalent circuit of the used coupled-inductor with shorted secondary winding.

Fig. 1(a), in which $k = \infty$, it is of importance to consider the following design guidelines:

- minimizing the leakage inductance using an interleaved winding approach in order to minimize the magnetizing current;
- minimizing the secondary winding resistance in order to minimize the magnetizing current and the power losses;
- using a small ferrite core with the highest possible permeability in order to minimize the number of turns and maximize the magnetizing inductance;
- using a small range hall effect current sensor (i.e. less than 1 A, which is available in the market) in order to maximize the measurement accuracy;
- designing the coupled-inductor with the possibility of having a small dc current in order to avoid magnetic core saturation.

It is worth to note that small range hall effect current sensors with different hole diameters up to 20 mm are available in the market, like LEM CTSR 0.3-P, whose hole diameter is equal to 20.3 mm. Using this sensor, two AWG 00 wires can be taken through it, where the equivalent maximum current is equal to 270 A, assuming an ampacity of 4 A/mm².

III. PV INVERTER CONTROL SCHEME IN GRID-TIED MODE WITH THE PROPOSED TECHNIQUE

Grid-tied PV inverters are commonly controlled using two control schemes. The first one is based on a proportional-integral (PI) current controller in the synchronous reference frame [25], [26], while the second one is based on a proportional-resonant (PR) or a proportional-integral-resonant (PIR) current controller in the stationary reference frame [27]–[29]. In this paper, a single loop PIR current controller is used, whose block diagram is shown in Fig. 2 [29].

Using the single loop PIR current controller, the current controller is given by

$$G_{PIR}(s) = K_P + \frac{K_I}{s} + \frac{K_R \cdot s}{s^2 + \omega_1^2}, \quad (3)$$

where K_P , K_I , and K_R are the proportional, integral, and resonant gains respectively. The integral term in this controller is used to regulate the dc current component [29]. Hence, if the proposed measurement technique is used as shown in Fig. 2, two parallel current controllers are utilized: the first one is a

TABLE I
PARAMETERS OF THE IMPLEMENTED DC CURRENT COMPONENT MEASUREMENT BOARD

Coupled-inductor	A	B
L_m (mH)	1.379	1.349
L_{l_s} (μ H)	0.525	0.522
R_s (m Ω)	37.7	39.7
k	11.5	10.68
I_s/I_p (p.u.)	0.996	0.9956
φ_s (rad)	0.0276 π	0.0297 π
I_m/I_p (p.u.)	0.0866	0.0932
φ_m (rad)	-0.472 π	-0.47 π

proportional-resonant (PR) current controller, whose transfer function is given by

$$G_{PR}(s) = K_P + \frac{K_R \cdot s}{s^2 + \omega_1^2}, \quad (4)$$

while the second one is an integral current controller (i.e. $G_I(s) = K_I/s$), where this controller is used only to control the dc current component, considering the measured dc values using the proposed technique. This controller has a low bandwidth in order to avoid any instability due to the measured residual ac component with the dc one using the proposed technique. Moreover, low pass filters can be used to effectively mitigate this small residual ac component. Notice that in Fig. 2, the dc current is measured in only two phases, but in a grounded system the third phase should be measured as well.

IV. EXPERIMENTAL VERIFICATION

In order to verify and evaluate the proposed technique, a dc current component measurement board has been designed and implemented as shown in Fig. 3. This board comprises two sets of the proposed dc current measuring unit (A and B), where each set has a 1:1 coupled-inductor combined with a hall effect current sensor in order to measure the dc component in a 5 kVA three-phase three-wire grid-tied system. Each coupled-inductor utilizes an RM 14 ungapped ferrite core, whose material is N41, and a CT 0.4-P hall effect LEM current sensor, where the nominal measuring range is equal to ± 400 mA. Table I summarizes the measured parameters of the two coupled-inductors shown in Fig. 3, where these parameters are measured using KEYSIGHT E4990A impedance analyzer.

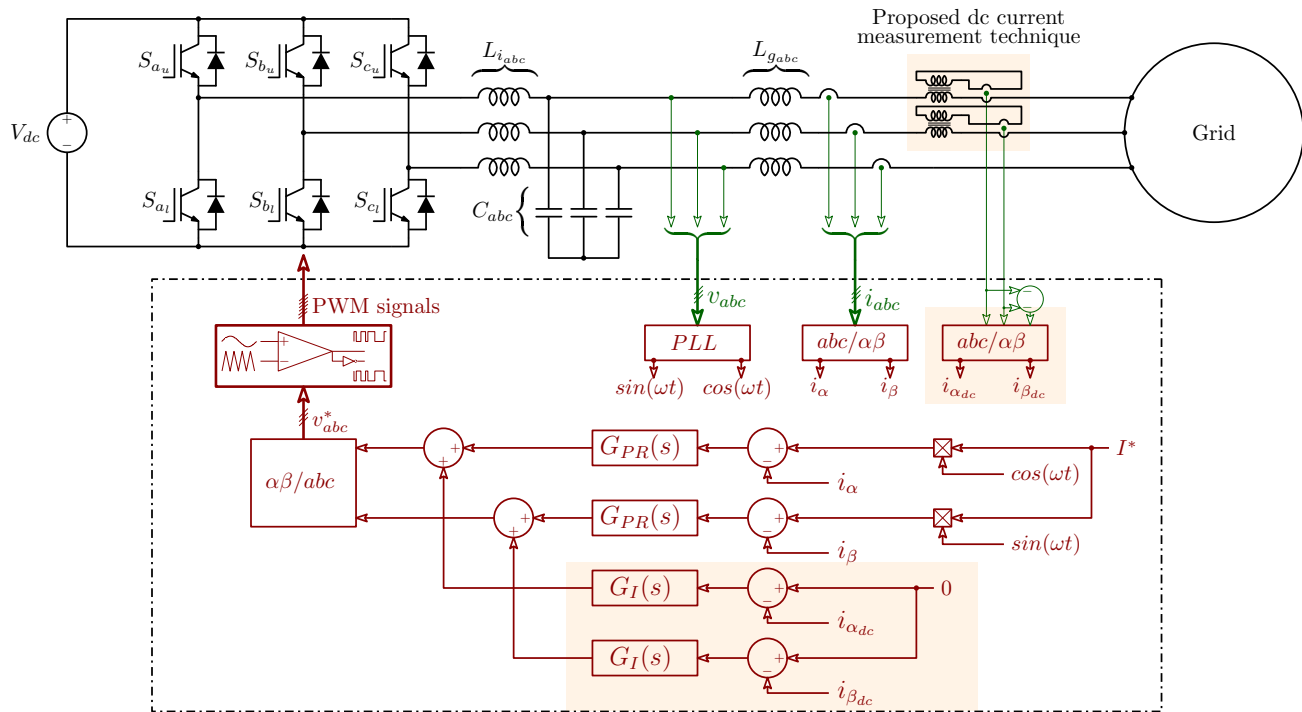


Fig. 2. Control scheme of a grid-tied three-phase three-wire voltage source inverter (VSI) using a proportional-integral-resonant (PIR) current controller, in which the proposed dc current component measurement technique is utilized considering two-phases.

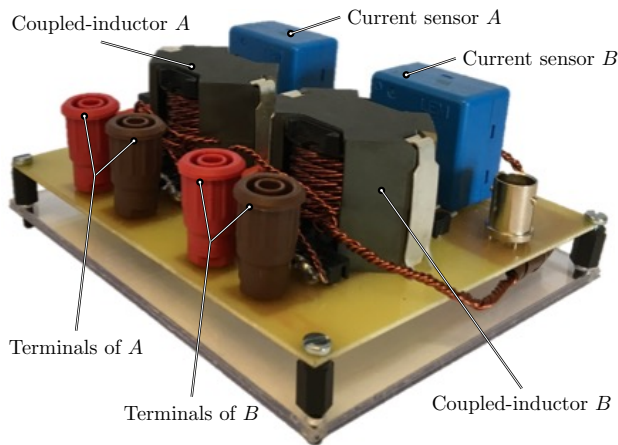


Fig. 3. Implementation of the proposed dc current component measurement technique for a 5 kVA three-phase three-wire grid-tied system.

Furthermore, the estimated residual ac component, which is measured with the dc one, (i.e. I_m/I_p) is calculated as shown in Table I using the prior equations.

The implemented dc current component measurement board, as shown in Fig. 3, has been tested separately in order to validate the introduced concept. At first an ac current is passed through the primary winding, and the current in the secondary winding and the sensor output are measured as shown in Fig. 4(a). Then, a small dc current has been passed through the primary winding, and the current in the secondary winding and the sensor output are measured again as shown in Fig. 4(b). These figures confirm the proposed concept and

shows the possibility of detecting a few milliamperes of dc current easily and with high accuracy. Note that there is an RC filter after the sensor output which is increasing the phase angle of the residual ac component and reducing its amplitude. Moreover, the low frequency component in the secondary current in Fig. 4(b) is due to the measurement noise in the current probe.

Finally, this board has been used in a 5 kVA three-phase three-wire grid-tied VSI. The control scheme of this inverter is as shown in Fig. 2. This prototype is utilized in order to examine the functionality of the proposed measurement technique. The dc current component is measured twice in the different phases using a KinetiQ PPA5530 power analyzer with and without the proposed measurement technique, where in the latter case a PIR current controller is utilized (i.e. an integral term has been added to limit the dc component). Fig. 5 shows the obtained measurements, in which the dc component has been effectively mitigated using the proposed measurement technique. Note that the added losses using the proposed board can be calculated as discussed before for one coupled-inductor from ($P_w = I_p^2 \cdot R_p + I_s^2 \cdot R_s \approx I^{*2} \cdot R_s$), where R_p is equal to R_s and I^* is the reference peak phase current. Hence, at full-load when $I^* = 7.58\sqrt{2}$ A, the power losses in the two coupled-inductors (A and B) are equal to 4.3 W and 4.54 W respectively, which represent 0.177% of the full-load power.

V. CONCLUSION

This paper has proposed a coupled-inductor-based dc current component measurement technique for transformerless grid-tied inverters. The merits behind this method are low cost,

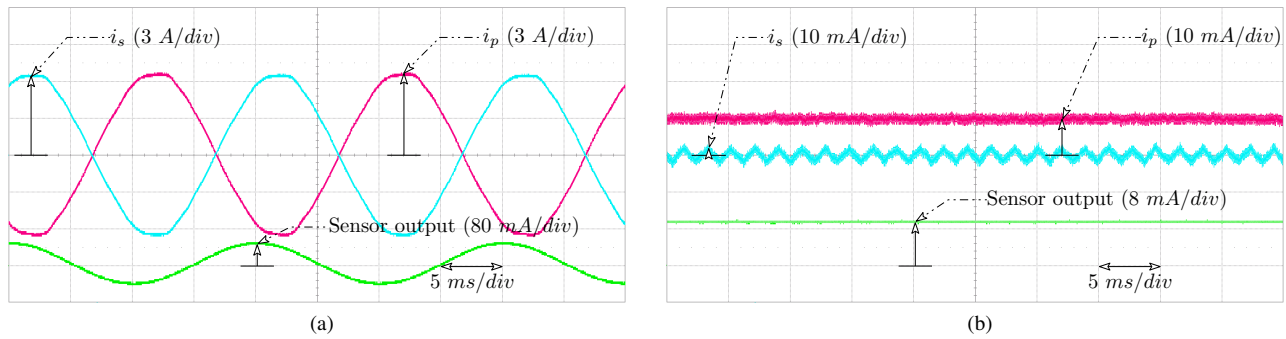


Fig. 4. Experimental results of testing the implemented dc current component measurement board, where the current through the primary and the secondary windings, and the sensor output are shown. (a) considering an ac current component in the primary winding; (b) considering a dc current component in the primary winding.

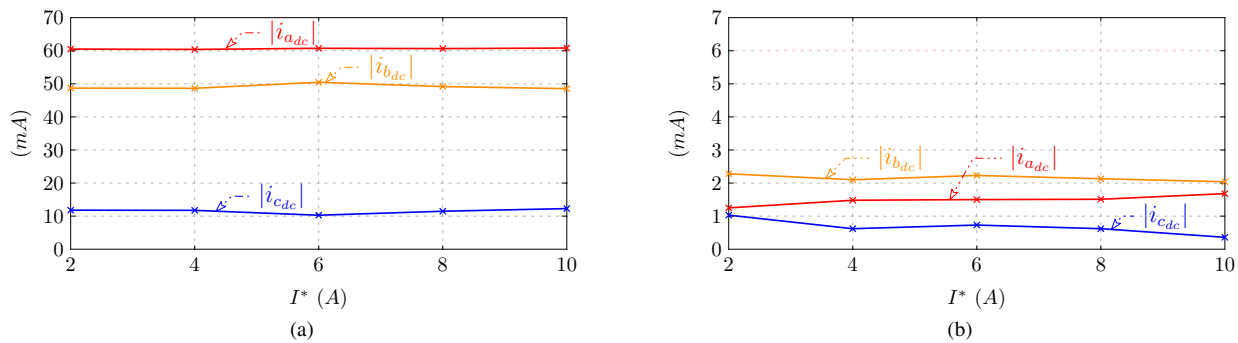


Fig. 5. Experimental results of the measured dc current component in the different phases. (a) without the proposed technique, where a PIR current controller is used; (b) with the proposed technique using the control scheme shown in Fig. 2.

simplicity, and high accuracy. Meanwhile, additional current sensors are used, but these sensors has a small range. Unlike all the conventional measurement techniques, the proposed one is able to measure the dc component itself, i.e. it does not predict its value from the measured dc offset between the inverter outputs. The proposed measurement technique is verified experimentally and tested in a 5 kVA three-phase three-wire transformerless grid-tied voltage source inverter, in which the dc component has been effectively reduced from 60 mA to 2 mA.

REFERENCES

- [1] M. Calais, V. G. Agelidis, and M. S. Dymond, "A cascaded inverter for transformerless single-phase grid-connected photovoltaic systems," *Renewable Energy*, vol. 22, no. 1, pp. 255–262, 2001.
- [2] W. Li, Y. Gu, H. Luo, W. Cui, X. He, and C. Xia, "Topology review and derivation methodology of single-phase transformerless photovoltaic inverters for leakage current suppression," *IEEE Trans. on Ind. Electron.*, vol. 62, no. 7, pp. 4537–4551, July 2015.
- [3] R. Gonzalez, E. Gubia, J. Lopez, and L. Marroyo, "Transformerless single-phase multilevel-based photovoltaic inverter," *IEEE Trans. on Ind. Electron.*, vol. 55, no. 7, pp. 2694–2702, July 2008.
- [4] E. Koutroulis and F. Blaabjerg, "Design optimization of transformerless grid-connected pv inverters including reliability," *IEEE Trans. on Power Electron.*, vol. 28, no. 1, pp. 325–335, Jan 2013.
- [5] Q. Yan, X. Wu, X. Yuan, Y. Geng, and Q. Zhang, "Minimization of the dc component in transformerless three-phase grid-connected photovoltaic inverters," *IEEE Trans. on Power Electron.*, vol. 30, no. 7, pp. 3984–3997, July 2015.
- [6] W. Li, L. Liu, T. Zheng, G. Huang, and H. Shi, "Research on effects of transformer dc bias on negative sequence protection," in *Int. Conf. on Advanced Power System Automation and Protection*, vol. 2, Oct 2011, pp. 1458–1463.
- [7] M. A. S. Masoum and P. S. Moses, "Impact of balanced and unbalanced direct current bias on harmonic distortion generated by asymmetric three-phase three-leg transformers," *IET Electric Power Applic.*, vol. 4, no. 7, pp. 507–515, August 2010.
- [8] F. Berba, D. Atkinson, and M. Armstrong, "A review of minimisation of output dc current component methods in single-phase grid-connected inverters pv applications," in *2nd Int. Symp. on Environm.Friendly Energies and Applic. (EFEA)*, June 2012, pp. 296–301.
- [9] "IEEE standard for interconnecting distributed resources with electric power systems," *IEEE Std 1547-2003*, pp. 1–28, July 2003.
- [10] "Reference technical rules for the connection of active and passive users to the lv electrical utilities," *Norma Italiana CEI 0-21*, pp. 1–156, Sept 2014.
- [11] W. M. Blewitt, D. J. Atkinson, J. Kelly, and R. A. Lakin, "Approach to low-cost prevention of dc injection in transformerless grid connected inverters," *IET Power Electron.*, vol. 3, no. 1, pp. 111–119, January 2010.
- [12] R. Sharma, "Removal of dc offset current from transformerless pv inverters connected to utility," in *40th Int. Universities Power Engineering Conf. (AUPEC)*, Sept 2005, pp. 1–5.
- [13] T. Ahfock and L. Bowtell, "Dc offset elimination in a single-phase grid-connected photovoltaic system," in *16th Australasian Universities Power Engineering Conf. (AUPEC)*, Dec 2006, pp. 1–6.
- [14] L. Bowtell and A. Ahfock, "Direct current offset controller for transformerless single-phase photovoltaic grid-connected inverters," *IET Renewable Power Gen.*, vol. 4, no. 5, pp. 428–437, September 2010.
- [15] T. Zhang, G. He, M. Chen, and D. Xu, "A novel control strategy to suppress dc current injection to the grid for three-phase pv inverter," in *Int. Power Electron. Conf. (IPEC-ECCE ASIA)*, May 2014, pp. 485–492.
- [16] G. He, D. Xu, and M. Chen, "A novel control strategy of suppressing dc current injection to the grid for single-phase pv inverter," *IEEE Trans. on Power Electron.*, vol. 30, no. 3, pp. 1266–1274, March 2015.
- [17] G. Buticchi, E. Lorenzani, and G. Franceschini, "A dc offset current compensation strategy in transformerless grid-connected power converters," *IEEE Trans. on Power Delivery*, vol. 26, no. 4, pp. 2743–2751, Oct 2011.

- [18] F. Berba, D. Atkinson, and M. Armstrong, "A new approach of prevention of dc current component in transformerless grid-connected pv inverter application," in *IEEE 5th Int. Symp. on Power Electron. for Distributed Generation Systems (PEDG)*, June 2014, pp. 1–7.
- [19] M. Armstrong, D. J. Atkinson, C. M. Johnson, and T. D. Abeyasekera, "Auto-calibrating dc link current sensing technique for transformerless, grid connected, h-bridge inverter systems," *IEEE Trans. on Power Electron.*, vol. 21, no. 5, pp. 1385–1393, Sept 2006.
- [20] G. A. Kern, "DC injection and even harmonics control system," United States Patent 6,282,104, Aug. 28, 2001.
- [21] S. N. Vukosavic and L. S. Peric, "High-Precision Sensing of DC Bias in AC Grids," *IEEE Trans. on Power Deliv.*, vol. 30, no. 3, pp. 1179–1186, June 2015.
- [22] S. N. Vukosavic and L. S. Peric, "High-Precision Active Suppression of DC Bias in AC Grids by Grid-Connected Power Converters," *IEEE Trans. on Industrial Electron.*, vol. 64, no. 1, pp. 857–865, Jan 2017.
- [23] N. Pjevalica and N. Petrovic and V. Pjevalica and N. Teslic, "Experimental Detection of Transformer Excitation Asymmetry through the Analysis of the Magnetizing Current Harmonic Content," *Elektronika ir Elektrotechnika*, vol. 22, no. 2, pp. 43–48, 2016.
- [24] R. Nalepa and F. Grecki and M. Ostrogorska and P. Aloszko and J. Duc, "DC-bias current measurement in high power AC grids," in *IEEE 15th European Conf. on Power Electron. and App. (EPE)*, Sept 2013, pp. 1–5.
- [25] F. Blaabjerg, A. Isidori, and F. M. Rossi, "Impact of modulation strategies on power devices loading for 10 MW multilevel wind power converter," in *IEEE 3rd Int. Symp. on Power Electron. for Distributed Generation Systems (PEDG)*, June 2012, pp. 751–758.
- [26] A. Abdelhakim, P. Mattavelli, V. Boscaino, and G. Lullo, "Decoupled control scheme of grid-connected split-source inverters," *IEEE Trans. on Ind. Electron.*, vol. PP, no. 99, pp. 1–1, 2017.
- [27] C. Bao, X. Ruan, X. Wang, W. Li, D. Pan, and K. Weng, "Step-by-step controller design for lcl-type grid-connected inverter with capacitor current-feedback active-damping," *IEEE Trans. on Power Electron.*, vol. 29, no. 3, pp. 1239–1253, March 2014.
- [28] Y. Tang, C. Yoon, R. Zhu, and F. Blaabjerg, "Generalized stability regions of current control for lcl-filtered grid-connected converters without passive or active damping," in *IEEE Energy Conversion Congress and Exposition (ECCE)*, Sept 2015, pp. 2040–2047.
- [29] D. Stojic, M. Milinkovic, S. Veinovic, and I. Klasnic, "Novel proportional-integral-resonant current controller for three phase pwm converters," in *4th Int. Symp. on Environmental Friendly Energies and Applic. (EFEA)*, Sept 2016, pp. 1–4.